ELSEVIER

Surface Science 392 (1997) 44–51

surface science

Area determination in fractal surfaces of Pt and Pt–Ru electrodes

V. Lakshminarayanan [a,1], R. Srinivasan [a,*], D. Chu [b], S. Gilman [b]

[a] *Applied Physics Laboratory, The Johns Hopkins University, Laurel, MD 20723-6099, USA*

[b] *Sensors and Electron Devices Directorate, Electrochemistry Branch Army Research Laboratory, Fort Monmouth, NJ 07703-5601, USA*

Received 5 March 1997; accepted for publication 6 June 1997

Abstract

A fractal approach using corrugation data to calculate surface area is offered as an alternative to gas adsorption technique. The surfaces of mechanically polished polycrystals of pure Pt and Pt–Ru(40%) alloy were examined using scanning tunneling microscopy. Over a range of 0.01–10 μm lengths, three fractal dimensions were identified. Measurements made at randomly selected locations separated by distances > 0.1 mm showed the existence of the three domains everywhere. However, in each domain, the fractal dimensions, D, varied from one location to another, suggesting a stochastic distribution of D. The stochastic data was used to calculate the surface area. In the pure Pt case, the area calculated on this basis correlated well with the area measured by the anodic stripping of adsorbed hydrogen. The usefulness of the fractal approach to area calculation in the Pt–Ru alloy, where the hydrogen absorption technique cannot be used, is demonstrated. © 1997 Elsevier Science B.V.

Keywords: Catalysis; Electrochemical methods; Fractal; Platinum; Ruthenium; Scanning tunneling microscopy; Surface roughness

1. Introduction

Surface area estimation in catalysts has long been made using adsorption–desorption techniques. In the case of Pt catalyst, a standard method of estimating the surface area is to determine the charge associated with anodic stripping of adsorbed hydrogen [1]. This technique cannot be used on catalysts such as Pd or Pt–Ru alloys, which absorb hydrogen into the metal lattice [2]. In this work we have demonstrated an alternate method to determine the surface area that does not involve the use of hydrogen or any other gas. It is based on the corrugation (z-axis) information obtained from scanning tunneling microscopy (STM), and can, in principle, be used for in situ monitoring of time-dependent changes of the surface area during the course of the surface reactions.

Most catalysts, including Pt and Pt–Ru, have a rough surface that exhibits a near fractal behavior [3,4]. Within a given location, their surfaces can exhibit more than one fractal dimension, as is demonstrated in this work. Furthermore, these surfaces are not homogeneously rough at all locations. STM has a fairly wide spatial resolution (0.01–500 nm or more), well over the diameters of hydrogen and most other gas-phase molecules used in adsorption techniques, and is thus ideally suited to study fractal surfaces. The STM tip can also be moved from one location to another to obtain a statistical average of the surface area.

* Corresponding author. Fax: (+1) 301 953.6904.

[1] Present address: Raman Research Institute, Bangalore—560 080, India.

PII S0039-6028(97)00458-5

In this work, we have used a mechanically roughened polycrystalline Pt disk as a model surface to demonstrate the capability of the STM-based fractal approach to determine its area. We have verified the validity of this approach by measuring the area through adsorption and anodic stripping of hydrogen in an aqueous acid medium. We have also measured the surface area of a roughened polycrystalline Pt–Ru alloy with the STM-based fractal technique.

2. Experimental procedure

2.1. Surface preparation

The surfaces of a Pt disc (99.999% purity; Johnson Matthey) and a polycrystalline Pt–Ru alloy (40% Ru by weight) prepared from 99.95% pure elements by arc-melting, were cleaned and roughened as follows. The disc-shaped samples were cleaned ultrasonically in triple distilled water. The surface of the electrodes were polished on a Buehler microcloth sequentially with 1.0, 0.3, 0.05 μm alumina and water. Then they were rinsed and cleaned ultrasonically with triple distilled water. They were polished again (or roughened), first with 1 μm, and then with 0.3 μm alumina, and rinsed and cleaned again ultrasonically with triple distilled water. Next, they were ultrasonically cleaned for 3 min in the test electrolyte (0.5 M H_2SO_4).

2.2. Electrochemical measurements

Cyclic voltammetry measurements were carried out in an air-sealed all-glass cell. The cell had three separate compartments for the working, counter and reference electrodes; fine porous glass frets were used as separators. A platinum gauze (99.999%) formed the counter-electrode. A reversible hydrogen electrode (RHE) served as the reference electrode; details of the fabrication of the RHE are described elsewhere [5]. An aqueous solution of 0.5 M H_2SO_4 (ultra-high-purity grade, Ultrex, J.T. Baker), which formed the electrolyte, was deaerated in the cell by bubbling ultrahigh purity argon (99.999%, Matheson), prior to the introduction of the working electrode. During the measurements, the solution was not bubbled, but the surface of the electrolyte was masked with argon to prevent dissolution of air. The geometric area of the electrodes exposed to the electrolyte were 0.83 cm^2 for Pt and 0.64 cm^2 for Pt–Ru. All measurements were performed at room temperature ($21 \pm 1^{\circ}C$). The instrumentation included an EG and G PAR 173 potentiostat, a EG and G PAR 175 programmer and a HP 7047A X–Y recorder.

For both Pt and Pt–Ru electrodes, cyclic voltammetric measurements were made using a scan rate of 10 mV s^{-1}. In the Pt–Ru case, potential scans were limited to between 0.04 and 0.6 V; this was necessary to minimize possible anodic dissolution of Ru at potentials more positive than 0.6 V. In the case of the Pt, the electrode was initially scanned between 0.04 and 1.5 V for five times. After the third scan, the current peaks in the hydrogen adsorption–desorption regions were reproducible. The sixth and the final scan was then performed only between 0.04 and 0.6 V. The hydrogen peaks in the fifth scan (scan range: 0.04–1.5 V) and the sixth scan (scan range: 0.04–0.6 V) matched well.

2.3. STM imaging

STM images in air, under constant current mode, were obtained to estimate the surface area of the Pt and the Pt–Ru electrodes. First, within a location of 10×10 μm, a sequence of images was obtained in progressively diminishing sizes down to 0.01×0.01 μm. Next, 30 images of 0.0562×0.0562 μm were obtained at different locations, that were randomly selected throughout the sample. Each image had 200×200 pixels, and the resolution was in the range of 0.05 μm (for the 10×10 μm image) to 0.00005 μm (for the 0.01×0.01 μm image). All images were square shaped. The tunneling current (10 nA) and the tip-sample bias voltage (0.1 V) were kept constant for all the images. The STM images were obtained ex situ by a Nanoscope II scanning tunneling microscope, immediately after the cyclic voltammetry measurements.

3. Results and discussion

3.1. Area measurements from anodic stripping of adsorbed hydrogen

Fig. 1 shows the cyclic voltammogram (CV) of the Pt (solid curve) and Pt–Ru (dashed curve) electrodes in aqueous, deaerated 0.5 M H_2SO_4; the current values shown in the figure are as measured and not corrected for the surface area. For Pt, the two peaks seen at 0.125 V and 0.275 V during the anodic cycle correspond to the stripping of the adsorbed hydrogen. The flat region between 0.35 and 0.60 V corresponds to the double layer region. The charge associated with the area under the anodic stripping of hydrogen is 280 μC (corrected for the charging of the double layer), which corresponds to a true surface area of 1.33 cm^2. This true surface area is based on the 210 μC cm^{-2} for the hydrogen adsorption/desorption reaction [1]. The CV for the Pt–Ru(40%) electrode, also in 0.5 M H_2SO_4, is shown in Fig. 1 (dashed curve). This result is in general agreement with those reported in the literature [6]. The net charge associated with the stripping of hydrogen is 146 μC. However, unlike the Pt electrode, the surface area of Pt–Ru electrode cannot be computed using the charge associated with the anodic stripping of hydrogen [2]. In this work, therefore, we did not use the charge data from the CV to calculate the surface area of the Pt–Ru electrode.

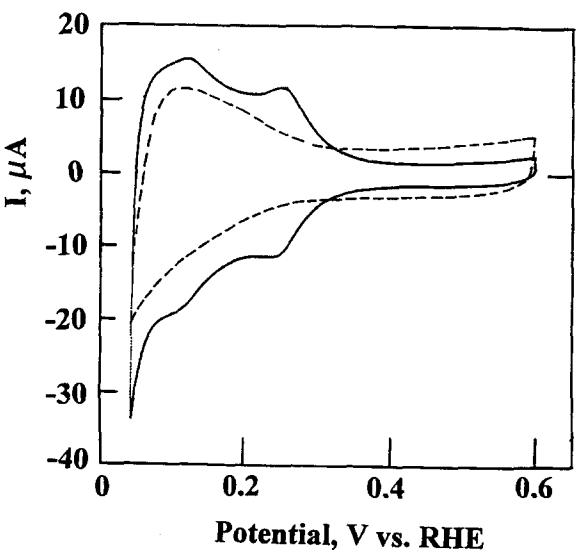

Fig. 1. Cyclic voltammograms in aqueous deaerated 0.5 M H_2SO_4 for polycrystalline electrodes: pure Pt (solid curve), and Pt–Ru(40%) alloy (dashed curve). Scan rate: 10 mV s^{-1}. The surfaces of both electrodes were roughened by 0.3 μm alumina.

3.2. The fractal approach to surface area calculation

The topographical features of the pure Pt surface, as obtained by STM, were similar at all resolutions within the 0.01–10 μm range. Two representative images obtained at two different magnifications are shown in Fig. 2a and b; the corresponding resolutions are 0.00028 and 0.028 μm. We treat this as a fractal surface. The similarities in the appearance at various levels of the magnification suggest that it is a self-similar surface. Since the active surface appears to be a continuous one, and not connected through islands of inactive areas, it is not a self-affine surface.

For each image, the surface area A was calculated using a triangulation technique [7]. All the surface area values were rescaled to the size of the largest image (10×10 μm) as $A' = A(10/l)^2$; where l is the length of the image in μm.

An important test for fractal surfaces (of square shaped objects) is the relationship between their area A and perimeter p [8]: $A^{0.5} \propto p^{1/D}$, where D is the fractal dimension. For an object with Euclidean geometry, $D=1$, in which case the perimeter, p will exactly be equal to $4\sqrt{A}$. Most surfaces will obey the condition of $D=1$, when the resolution(s) of the scale or the yardstick used in the measurement is comparable with l. Under the condition when $s \ll l$, the value of D may deviate from 1. A surface which exhibits a $D>1$ for $s \ll l$ is said to be fractal in dimension D.

Fig. 3 shows a $\log A$ vs. $\log p$ plot for the polycrystalline Pt, over a range of l, from 0.01–10 μm. As described in Section 2, A was calculated using a triangulation technique on the STM data; the STM images were square shaped of length l. The solid line represents a linear regression fit over the entire range of p, and it yielded a D of 1.769 with a correlation coefficient

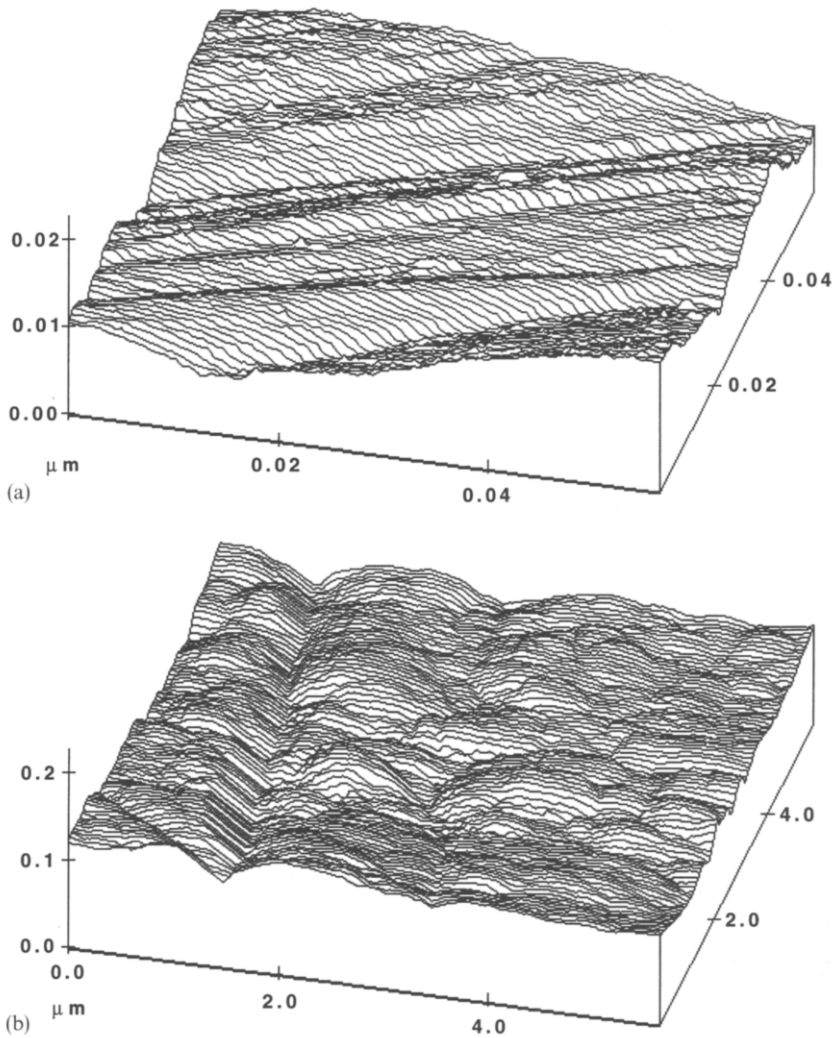

Fig. 2. STM images of the roughened Pt surface at resolutions of (a) 2.81×10^{-4} μm, and (b) 2.81×10^{-2} μm. Note that the two images have similar features, even at different levels of resolutions. The STM images were obtained at constant current mode with a bias voltage of 0.1 V and 10 nA tunneling current.

(R^2) of 0.987 [2]. However, as can be seen from this figure, the surface clearly exhibited more than one fractal behaviour. For $0.2 < l < 10$ μm, the linear regression fit yielded a $D = 1.001$ with an $R^2 = 0.999$; this section of the plot is designated Domain I in the figure. For $0.03\ \mu m < l < 0.2\ \mu m$, $D = 1.60$ with an $R^2 = 0.999$; this section of the plot is designated Domain II. For $l < 0.03$ μm, designated as Domain III the D value appears to be much larger, and was not estimated. The pixel sizes (or the resolution) of the STM images in Domain III were ≤ 1.5 Å, and comparable with or smaller than interatomic distances on the Pt surface.

[2] The data in Fig. 2 were obtained at a single location only for $0.01 < l < 0.562$ μm. For $l > 0.562$ μm, the data was obtained at a different location. The change of location was necessitated by the resolution of the STM head; in the Nanoscope II setup, one single head will not cover the entire range of l used in our experiment. Nevertheless, this did not appear to cause any serious discontinuity in the plot, perhaps because $D \to 1$ for $l > 0.2$ μm.

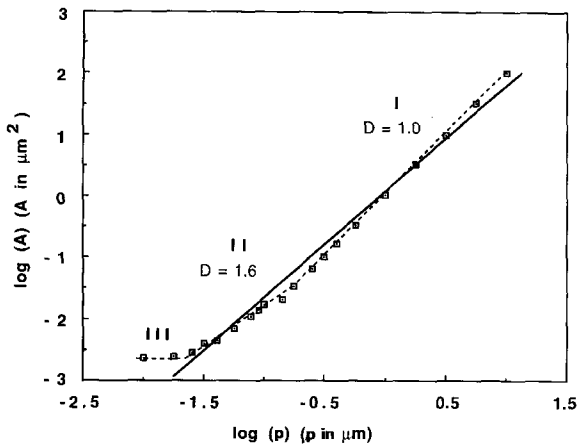

Fig. 3. Log A vs. log p plot for the roughened Pt surface, covering three orders of magnitude of length. The dotted lines represent three domains of fractal dimensions over the entire range. The solid line represents a forced linear regression over the entire range.

The fractal representation presented in Fig. 3 is of a conventional type [8]. We found that rescaling the A values to the size of the largest image (10×10 μm) as $A' = A(10/l)^2$, and plotting log A' vs. log s reveals the three fractal domains more clearly than the log A vs. log p plot, see Fig. 4. Further, the often quoted work by Mandelbrot [8], appears to suggest that within a given self-similar system (for example, the surface of the roughened Pt), there is only one fractal geometry,

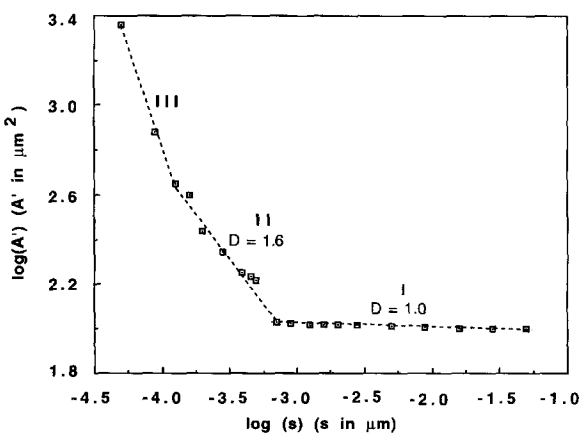

Fig. 4. Log A' vs. log s representation for the same data in Fig. 3. The three fractal domains can be more easily identified in this representation.

i.e., there is only one unique value for D. In contrast, the Pt data in Figs. 3 and 4 show the presence of more than one fractal geometry within the same surface. The Pt surface described in this work is by no means a unique case of a surface with more than one fractal dimension. Recent literature shows that plants [9], clouds [10,11], geological sediments [12], and several other systems [11] all exhibit more than one fractal dimension at different levels of magnifications.

The Pt surface discussed above not only exhibited more than one fractal dimension, but the areas at different locations of the surface, obtained at the same level of magnification, were not identical. The log A vs. log p plots obtained at different locations exhibited three distinct domains, as seen in Figs. 3 and 4. The D value in Domain I was very close to 1.001 reported in Fig. 3. However, within Domain II the value of D varied significantly from one location to another. In other words, the surface was not homogeneously rough. Similar results were also obtained on repeatedly roughened (0.3 μm alumina) pure Pt samples. Exposing the electrode to the electrolyte did not change its fractal properties.

For the purpose of surface area calculations, we assumed that contributions to the roughness from Domain I are insignificant. Contributions from Domain III, which are in the atomic and subatomic scales ($l \leq 20$ nm; $s \leq 0.1$ nm), were also not considered; there are no reactants that can be packed together in dimensions < 0.1 nm. The surface roughness observed in the 0.03×0.03–0.15×0.15 μm range was assumed to be the only contributing factor to the surface area.

Multiple images of an 0.0562×0.0562 μm image size were obtained at 30 different locations, randomly selected throughout the Pt surface; no two locations were separated by < 0.1 mm from each other. Fig. 5 shows the distribution plot or the histogram of the surface area, A, for the 30 locations. The distribution was approximated to Lorentzian, and the mean area was obtained as 0.0048 μm², which is about 1.5 times larger than the geometric area 0.00316 μm². A similar distributed approach to the area measurement, using different sizes of STM images within Domain II, gave ratios that were close to the 1.5 value. Using

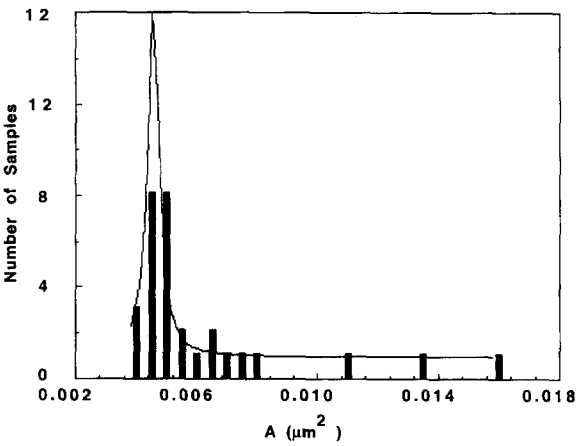

Fig. 5. Histogram of the surface area, A, obtained from the roughened Pt surface using STM images of 0.0562×0.0562 μm, with a resolution of 0.28 nm. The images were obtained at 30 randomly selected locations of the Pt electrode. The solid line corresponds to a Lorentzian fit.

this ratio, we calculated the surface area of the 0.83 cm^2 electrode as 1.24 cm^2. This is in good agreement with the 1.33 cm^2 surface area obtained from the anodic stripping data in Fig. 1.

3.3. Surface area of polycrystalline Pt–Ru(40%) alloy

Fig. 6 shows the $\log A$ vs. $\log p$ plot for the Pt–Ru alloy, which also shows three distinct

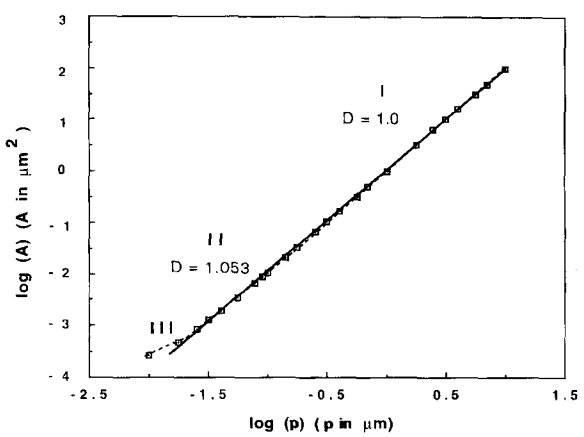

Fig. 6. Log A vs. log p plot for the roughened Pt–Ru (40%) surface. The dotted lines represent three domains of fractal dimensions over the entire range. The solid line represents a forced linear regression over the entire range.

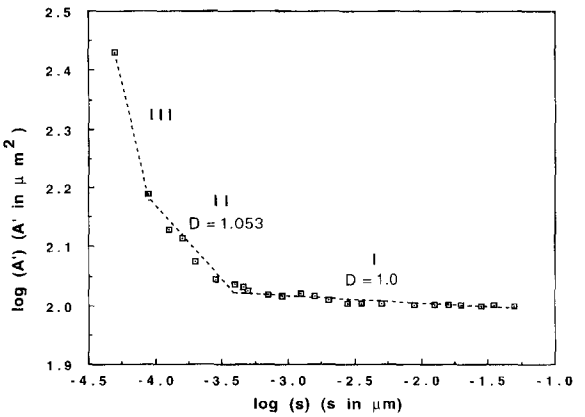

Fig. 7. Log A' vs. log s representation for the same data in Fig. 6. The three fractal domains can be more easily identified in this representation.

domains as in the pure Pt case; the distinction is more obvious in the $\log A'$ vs. $\log s$ plot in Fig. 7. In this case too, only Domain II showed a fractal dimension $D > 1$; Domain I has a $D = 1.0$. Domain III is attributed to atomic-scale corrugations, and not treated as fractal. Thus, it was assumed that the roughness that contributed to the surface area enhancement were within the 0.03×0.03–0.15×0.15 μm limits. As in the pure Pt case, in addition to the fractal property, the Pt–Ru surface also exhibited a heterogeneous roughness, i.e., the D values in each domain varied from one location to another. STM images were obtained, and surface areas were computed at 30 different locations (image size $= 0.0562 \times 0.0562$ μm), and the resulting histogram is shown in Fig. 8. This was approximated to a Lorentzian fit, and a mean area was obtained as 0.0042 μm^2. This is about 1.33 times larger than the geometric area. Thus, the true surface area of the 0.64 cm^2 (geometric area) Pt–Ru electrode is 0.85 cm^2.

4. Conclusions

The surfaces of pure Pt and Pt–Ru(40%) alloy, when roughened using 0.3 μm alumina, show three distinct domains of different fractal dimensions, D, over a range of 0.01–10 μm length. Surfaces measured with a resolution $s \geq 1$ nm have $D \rightarrow 1$,

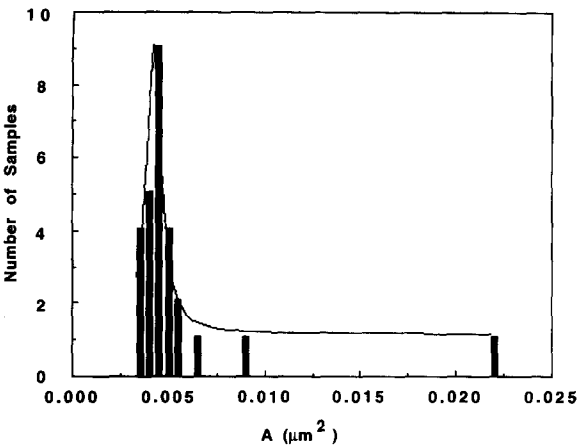

Fig. 8. Histogram of the surface area, A, obtained from the roughened Pt–Ru(40%) surface using STM images of 0.0562×0.0562 μm, with a resolution of 0.28 nm. The images were obtained at 30 randomly selected locations of the Pt–Ru(40%) electrode. The figure shows only 27 samples. Three samples with larger areas (0.0786, 0.0831 and 0.1786 μm^2) are outside the x-axis range, and have not been included in the figure. The solid line corresponds to a Lorentzian fit, and it includes all 30 samples.

and are termed Domain I. For measurement resolutions in the range 0.15–1.0 nm, the surface has $D>1$, and is termed Domain II. A third fractal dimension was also observed when $s<0.1$ nm, and is termed Domain III. The three domains were observed at any randomly selected locations that were separated by distances >0.1 mm. However, the values of D varied from one location to another, especially within Domain II. In the pure Pt case, the surface area calculated based on the surface roughness in Domain II correlated well with the surface area obtained by the anodic stripping of adsorbed hydrogen.

The fractal properties of several other electrochemical systems and interfaces have been studied in the past using STM and atomic force microscopy. For example, electrodeposits of gold and platinum [13] and roughened silver electrodes [14] have been reported to exhibit self-similar and self-affine fractal structures. Similar to those results, our work also confirms that roughened Pt and Pt–Ru electrodes exhibit fractal properties. In addition, we have shown that on a given surface there is a stochastic distribution of the fractal dimension, which we have used to determine the area of the macro surface. In the pure Pt case, we have also provided independent confirmation of the surface area through the measurement of anodic stripping of adsorbed hydrogen.

Use of electrochemical techniques such as chronoamperometry and a.c. impedance to determine fractal dimensions of rough and "blocked" electrodes has also been reported in the literature [15–18]. The fractal properties of a wide variety of porous surfaces have been modeled under various electrochemical conditions, namely, ideally polarized, partial activation controlled, and total diffusion limited. Of these, the electrochemical condition of total diffusion limited process appears to be most suitable for characterizing fractal dimensions, provided the surface roughness is comparable with the Nernst diffusion layer thickness, and in the 1–100 μm range [15]. If the surface reaction is under partial activation control, the electrochemical techniques may not provide accurate information about the fractal dimension of the surface [15–17]. Even under ideally polarizable conditions, where one would expect little or no interference from faradaic reactions, the applicability of electrochemical techniques to estimate fractal dimensions is far from resolved [18]. For the two systems (Pt and Pt–Ru) reported in this work, the impedance techniques may not be applicable for the following reasons. The surface roughness for these electrodes is on the order of 0.025–0.2 μm, which is much less than the typical diffusion layer thickness [15]. The Pt–Ru electrode has virtually no double layer region in the sulfuric acid medium, and may be under partial activation control at all potentials. The STM-based technique described in this work faces no such limitations, and is a desirable technique for determining the fractal dimensions and surface roughness of the Pt and Pt–Ru electrodes.

Acknowledgements

Financial assistance was provided by the Army Research Laboratory MRCP program. Dr. Fernando Pineda helped us with the fractal interpretation of the surface geometry. Editorial help

by Benjamin S. Walker is gratefully acknowledged. Dr. P. Gopalan helped prepare the arc-melted Pt–Ru alloy.

References

[1] (a) V.S. Bagotzky, T.B. Vassilyev, Electrochim. Acta 12 1323 (1967); (b) L. Bai, L. Gao, B.E. Conway, J. Chem. Soc., Faraday Trans. 89 (1993) 235; (c) B.E. Conway, H. Angerstein-Kozlowska, Acc. Chem. Res. 14 (1981) 49.

[2] (a) S. Hadzi-Jordanov, H. Angerstein-Kozlowska, B.E. Conway, J. Electroanal. Chem. 60 (1975) 359; (b) S. Hadzi-Jordanov, H. Angerstein-Kozlowska, B.E. Conway, J. Phys. Chem. 81 (1977) 2271.

[3] B. Sapoval, in: A. Bunde, S. Havlin (eds.), Fractals and Disordered Systems, Springer, New York, 1991, p. 207.

[4] (a) D. Avnir, D. Farin, P. Pfeirrer, J. Chem. Phys. 79 (1983) 3566; (b) D. Avnir, D. Farin, Nature 308 (1984) 261.

[5] D. Chu, S. Gilman, J. Electrochem. Soc. 141 (1994) 1770.

[6] (a) D. Chu, S. Gilman, J. Electrochem. Soc. 143 (1996) 1685; (b) B.D. McNicol, J. Electroanal. Chem. 118 (1981) 71; (c) H.A. Gasteiger, N. Markovic, P. Roos, Jr., E. Cairns, J. Phys. Chem. 97 (1993) 12020.

[7] G.A. Korn, T.M. Korn (eds.), Mathematical Handbook of Scientists and Engineers, McGraw-Hill, New York, 1961, p. 54.

[8] B.B. Mandelbrot (ed.), The Fractal Geometry of Nature, W.H. Freeman, New York, 1982, p. 109.

[9] D.R. Morse, J.H. Lawton, M.M. Dodson, M.H. Williamson, Nature 314 (1985) 731.

[10] S. Lovejoy, Science 216 (1982) 185.

[11] J.-P. Rigaut in: G. Cherbit (eds.), Fractals: Non-integral Dimensions and Applications, Wiley, New York, 1990, p. 151.

[12] J.D. Orford, W.B. Whalley, Sedimentology 30 (1982) 655.

[13] J.M. Gomez-Rodriguez, A.M. Baro, L. Vazquez, R.C. Salvarezza, J.M. Vara, A.J. Arvia, J. Phys. Chem. 96 (1992) 347.

[14] I. Otsuka, T. Iwasaki, J. Vac. Sci. Technol. B 14 (1996) 1153.

[15] T. Pajkossy, A.P. Borosy, A. Imre, S.A. Martemyanov, G. Nagy, R. Schiller, L. Nyikos, J. Electroanal. Chem. 366 (1994) 69 and references cited therein..

[16] T. Pajkossy, L. Nyikos, Phys. Rev. B 42 (1990) 709 and references cited therein.

[17] (a) R. de Levie, J. Electroanal. Chem. 281 (1990) 1; (b) B. Kurtyka, R. de Levie, J. Electroanal. Chem. 322 (1992) 63.

[18] (a) M. Keddam, H. Takenouti, Electrochim. Acta 33 (1988) 445; M. Keddam in Fractals: G. Cherbit (ed.), Non-integral Dimensions and Applications, Wiley, New York, 1990, p. 135.